JMEPEG (2016) 25:1336–1341
DOI: 10.1007/s11665-016-1987-6

1059-9495/$19.00

Microstructure and Precipitate's Characterization of the Cu-Ni-Si-P Alloy

Yi Zhang, Baohong Tian, Alex A. Volinsky, Huili Sun, Zhe Chai, Ping Liu, Xiaohong Chen, and Yong Liu

(Submitted December 4, 2015; in revised form February 4, 2016; published online March 3, 2016)

Microstructure of the Cu-Ni-Si-P alloy was investigated by transmission electron microscopy (TEM). The alloy had 551 MPa tensile strength, 226 HV hardness, and 36% IACS electrical conductivity after 80% cold rolling and aging at 450 °C for 2 h. Under the same aging conditions, but without the cold rolling, the strength, hardness, and electrical conductivity were 379 MPa, 216 HV, and 32% IACS, respectively. The precipitates identified by TEM characterization were δ-Ni_2Si. Some semi-coherent spherical precipitates with a typical coffee bean contrast were found after aging for 48 h at 450 °C. The average diameter of the observed semi-coherent precipitates is about 5 nm. The morphology of the fracture surface was observed by scanning electron microscopy. All samples showed typical ductile fracture. The addition of P refined the grain size and increased the nucleation rate of the precipitates. The precipitated phase coarsening was inhibited by the small additions of P. After aging, the Cu-Ni-Si-P alloy can gain excellent mechanical properties with 804 MPa strength and 49% IACS conductivity. This study aimed to optimize processing conditions of the Cu-Ni-Si-P alloys.

Keywords aging treatment, cold rolling, Cu-Ni-Si-P alloy, microstructure, physical properties

1. Introduction

Electronic packaging lead frame is an important part of integrated circuits. Lead frame alloys are required to have high strength and conductivity (Ref 1-5). Cu-Ni-Si alloys are widely used in lead frames because of their good electrical conductivity and high strength (Ref 6-10). In order to obtain better mechanical properties with lower conductivity loss, many types of Cu-Ni-Si alloys have been utilized, including Cu-Ni-Si-Ag (Ref 11), Cu-Ni-Si-Mg (Ref 12), Cu-Ni-Si-Co-Zr (Ref 13), Cu-Ni-Si-Zr (Ref 14), Cu-Ni-Si-Al (Ref 15), and Cu-Ni-Si-Zn (Ref 16). These alloys can gain high strength and conductivity by precipitation of hard secondary phases upon aging, such as Ni_2Si, Ni_3Al, Co_2Si, Ni_3Si, and Cr_3Si. Zhang et al. (Ref 11) have studied the Cu-Ni-Si-Ag alloy and found that the addition of Ag can refine the grain and optimize the hot workability of the Cu-Ni-Si alloy. Lei et al. (Ref 12) studied the Cu-8.0Ni-1.8Si-0.15Mg alloy and found that precipitates of β-Ni_3Si and δ-Ni_2Si occurred when the alloy was aged at 450 °C for 30 min. Krishna et al. (Ref 13) studied the Cu-Ni-Si-Co-Zr alloy and found that the hardness and electrical conductivity can reach 216 HV and 45% IACS upon aging at 500 °C for 3 h followed by air cooling. The increase in strength after aging is attributed to the precipitation of fine Ni_2Si and Co_2Si particles. Xiao et al. (Ref 14) have identified three kinds of precipitates resulting from spinodal decomposition and the δ-Ni_2Si phase with disk-like structure appearing in the (Ni, Si)-rich regions during aging of the Cu-2.1Ni-0.5Si-0.2Zr alloy. Shen et al. (Ref 15) found nano-scale Ni_3Al and Ni_2Si particles precipitated in the Cu-10Ni-3Al-0.8Si alloy during aging. Zhao et al. (Ref 16) studied the Cu-3.2Ni-0.75Si-0.3Zn alloy and found three different transformation products: a modulated structure resulting from spinodal decomposition, $(Cu, Ni)_3Si$ with DO_{22}-ordered structure nucleating from the modulated structure and the disk-like δ-Ni_2Si phase appearing in the (Ni, Si)-rich regions. However, there are little studies of the Cu-Ni-Si alloys with P addition, which can improve strength and conductivity.

A study of the phase transformations and physical properties of the Cu-Ni-Si-P alloy has been carried out in this paper. In addition, the influence of aging processes on strengthening is discussed in relation with the phase transformation mechanisms. Precipitates were characterized by electron microscopy and correlated with the alloy strength.

2. Experimental Details

The Cu-Ni-Si-P alloy was prepared with pure Cu, Ni, Si, and P by melting in a vacuum induction furnace under argon atmosphere, and then cast into a low-carbon steel mold with ϕ 83 mm × 150 mm dimensions. Its chemical composition in wt.% is as follows: 2% Ni, 0.5% Si, 0.03% P, and Cu balance. The ingot was homogenized at 850 °C for 2 h to remove segregation of the alloying elements. Subsequently, the ingot was forged into bars of 25 mm in diameter. The forged bars were solution treated at 950 °C for 1 h, followed by water

Yi Zhang, Baohong Tian, Huili Sun, and **Yong Liu**, School of Materials Science and Engineering, Henan University of Science and Technology, Luoyang 471003, China and Collaborative Innovation Center of Nonferrous Metals, Luoyang 471003 Henan, China; **Alex A. Volinsky**, Department of Mechanical Engineering, University of South Florida, Tampa 33620; **Zhe Chai**, School of Materials Science and Engineering, Henan University of Science and Technology, Luoyang 471003, China and School of Materials Science and Engineering, University of Shanghai for Science and Technology, Shanghai 200093, China; and **Ping Liu** and **Xiaohong Chen**, School of Materials Science and Engineering, University of Shanghai for Science and Technology, Shanghai 200093, China. Contact e-mails: zhshgu436@163.com and volinsky@eng.usf.edu.

quenching. The alloy was cold rolled with 40, 60, or 80% reduction. The aging temperature ranged from 400 to 500 °C. The aging treatment was carried out in argon in a tube electric resistance furnace with 5 °C temperature accuracy. Electrical resistance was measured using ZY9987-type micro-ohmmeter with measurement error of less than 1% IACS. Hardness was measured using HVS-1000-type hardness tester under a 200 g load and 5-s holding time. Hardness measurement accuracy is better than 1.5%. Tensile tests were carried out on a screw-driven SHIMADZU-AG-I 250 kN testing machine, and the tensile strength standard deviation meets the ASTM-E8 standard. The microstructure was investigated using a JSM JEOL-5610LV scanning electron microscope. All specimens were polished and then etched with a solution of $FeCl_3$ (5 g) + C_2H_5OH (85 mL) + HCl (10 mL). The samples for transmission electronic microscopy (TEM) characterization were prepared using a Gatan 691 ion beam thinner. The precipitated phase was identified using a JEM-2100 high-resolution transmission electron microscope (HRTEM).

3. Results and Discussion

3.1 Physical Properties

The variation in hardness of the alloy aged at 400, 450, and 500 °C is shown in Fig. 1(a). It can be seen that for a given temperature, the alloy hardness initially increases rapidly and then plateaus with aging time. The alloy shows peak hardness of 225 HV after 4 h aging at 450 °C and 208 HV after 4 h aging at 500 °C, respectively. For a given aging time, the hardness of the alloy aged at 450 °C is higher than that at 500 °C. This is because higher aging temperature and longer aging time lead to overaging (Ref 17).

Electrical conductivity curves of the alloy aged at 400, 450, and 500 °C are shown in Fig. 1(b). Due to the solute elements precipitating out of the supersaturated solution, electrical conductivity increased rapidly at the beginning of aging, and then increased slightly as the solute concentration in copper approached equilibrium. Electrical conductivity can reach 32% IACS for the alloy aged at 450 °C for 2 h and 30% IACS after 2 h aging at 500 °C, respectively.

Figure 2 shows the hardness and conductivity curves of the Cu-Ni-Si-P alloy aged at 450 °C for a different cold working prior to aging. The peak hardness increases with cold rolling reduction and reaches 226, 229, and 240 HV with 40, 60, and 80% cold rolling, respectively. The peak hardness is only 216 HV without cold rolling. Dislocations resulting from cold rolling act as diffusion paths for solute atoms and provide nucleation sites for precipitation during aging treatment (Ref 18). The greater the cold rolling, the higher the peak hardness is.

The change of conductivity of the alloy aged at 450 °C is shown in Fig. 2(b). It can be seen that the conductivity of the alloy increases rapidly during initial stages of the aging process. That is because the growth of precipitates reduces the amount of solute atoms in the matrix, and then the conductivity increases continuously during aging (Ref 19). For a given aging time, greater cold rolling leads to higher conductivity. With 0, 40, 60, and 80% cold rolling reduction, the alloy conductivity reached 32, 36, 38, and 41% IACS when aged at 450 °C for 2 h, respectively.

Variation in the tensile strength values of the alloy aged at 450 °C is shown in Fig. 3. With 40% cold rolling reduction, the alloy shows peak strength of 562 MPa when aged at 450 °C for 1 h and then the strength continuously decreased with aging time. This is due to overaging when the aging time is longer than 1 h. The strength is only 372 MPa without cold rolling after 1 h aging at 450 °C. Some research results show that the increase in strength obtained at cold rolling is due to increased dislocation density (Ref 11-15).

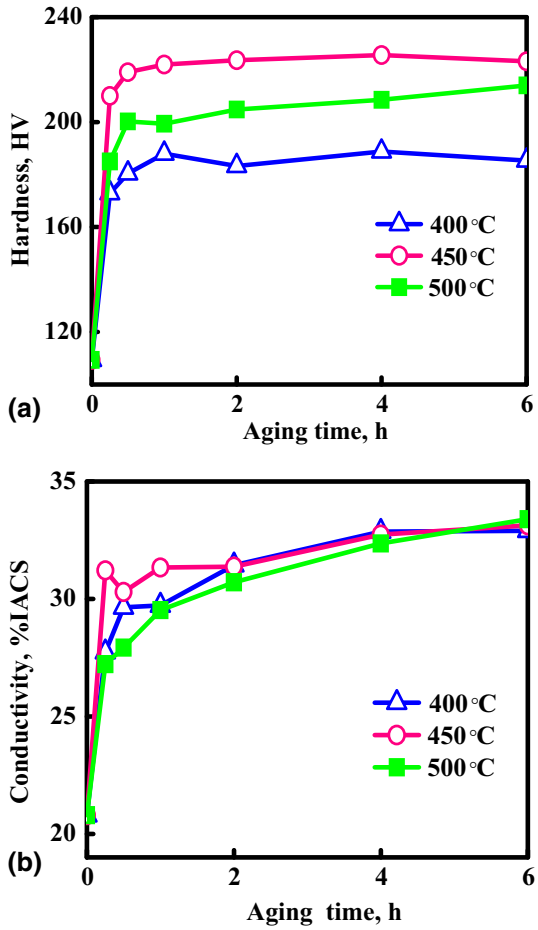

Fig. 1 Aging temperature effects on (a) the hardness and (b) conductivity of the Cu-Ni-Si-P alloy

Figure 4 shows the tensile fractographs of the alloy aged at 450 °C for 1 h. The morphology of the fracture surface was observed by SEM. All samples showed typical ductile fracture patterns. The precipitation particles were very hard and have been broken away from the matrix grains (Ref 20). Many shallow dimples were observed. It can be seen that the alloy with 40% cold rolling in Fig. 4(b) has more dimples than without cold rolling in Fig. 4(a). This is due to the higher number of precipitates at these conditions.

3.2 Microstructure Characterization

Transmission electron microscopy and selected area diffraction pattern (SADP) of the solution-treated alloy aged at 450 °C for 2 h and 48 h are shown in Fig. 5(a)-(c), respectively. Figure 5(a) and (b) shows that a large amount of nano-scale particles precipitated in the Cu matrix during aging. With increasing aging time, more precipitates were observed (Fig. 5b) and they gradually grew in size. Figure 5(b) illustrates the typical coffee bean contrast of some semi-coherent

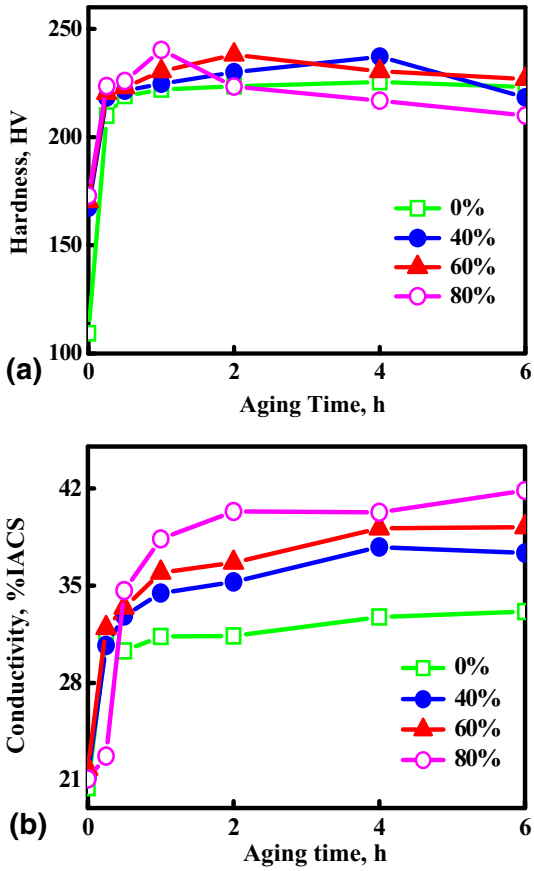

Fig. 2 Cold deformation effects on (a) the hardness and (b) conductivity of the Cu-Ni-Si-P alloy aged at 450 °C

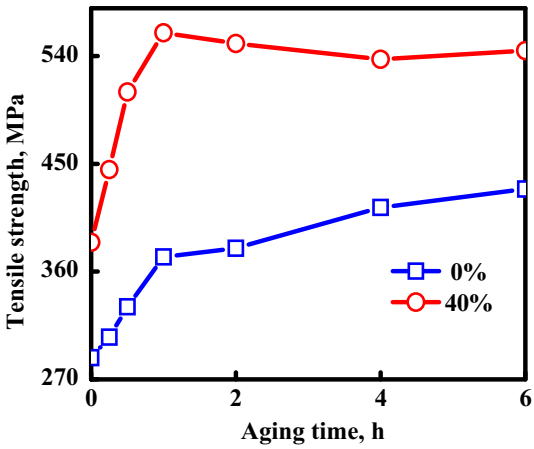

Fig. 3 Tensile strength of the Cu-Ni-Si-P alloy aged at 450 °C

spherical precipitates (marked by arrows) in the sample aged for 48 h at 450 °C. The average diameter of the observed semi-coherent precipitates is about 5 nm. Similar results were observed by Altenberger and Lockyer in Ref 21, 22. SADPs obtained from the precipitates are shown in Fig. 5(c). It can be seen that the precipitates identified in the present study were δ-Ni_2Si. It appears that these precipitates can act as obstacles to prevent dislocations movement during cold rolling. As a result, the alloy was strengthened effectively by the Orowan strengthening mechanism (Ref 23). Some researchers added different

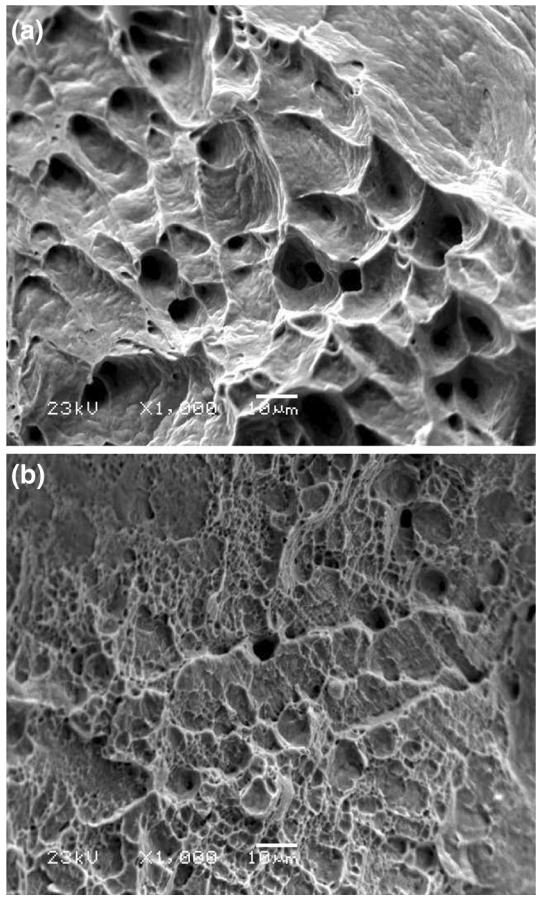

Fig. 4 Tensile-tested fracture surfaces of the Cu-Ni-Si-P alloy aged at 450 °C for 1 h: (a) no cold rolling and (b) 40% cold rolling

kinds of trace elements, such as Mg, Co, and Al into Cu-Ni-Si alloys. This can enhance the variety of precipitates (β-Ni_3Si and δ-Ni_2Si, Ni_2Si and Co_2Si, Ni_2Si and Ni_3Al) (Ref 12, 13, 15). However, small additions of P can have beneficial effects on the Cu-Ni-Si alloy properties. The addition of P can refine grain size and increase the nucleation rate of the precipitates, as shown in Fig. 7. Thus, the Cu-Ni-Si-P alloy can gain excellent mechanical properties.

HRTEM images and corresponding Fourier transform patterns of solution-treated Cu-Ni-Si-P alloy aged at 450 °C for 48 h are shown in Fig. 6. Fourier transform patterns of Fig. 6(b)-(d) show that the diffraction patterns came from the δ-Ni_2Si phase. To investigate if precipitates are coherent with the matrix, the misfit strain value of the precipitates can be calculated as (Ref 15):

$$\delta = 2\frac{d_p - d_m}{d_p + d_m}, \qquad \text{(Eq 1)}$$

where d_p and d_m are the plane spacing of the precipitation and the copper matrix, respectively.

$$\delta = 2\frac{d_{(002)_{\delta-N_2Si}} - d_{(002)_{Cu}}}{d_{(002)_{\delta-N_2Si}} + d_{(002)_{Cu}}} = 2\frac{1.8645 - 1.8075}{1.8645 + 1.8075} = 0.031. \qquad \text{(Eq 2)}$$

According to the obtained misfit strain, the misfit value between $(002)_{Cu}$ and $(002)_{\delta-Ni_2Si}$ was 0.031, which is less than

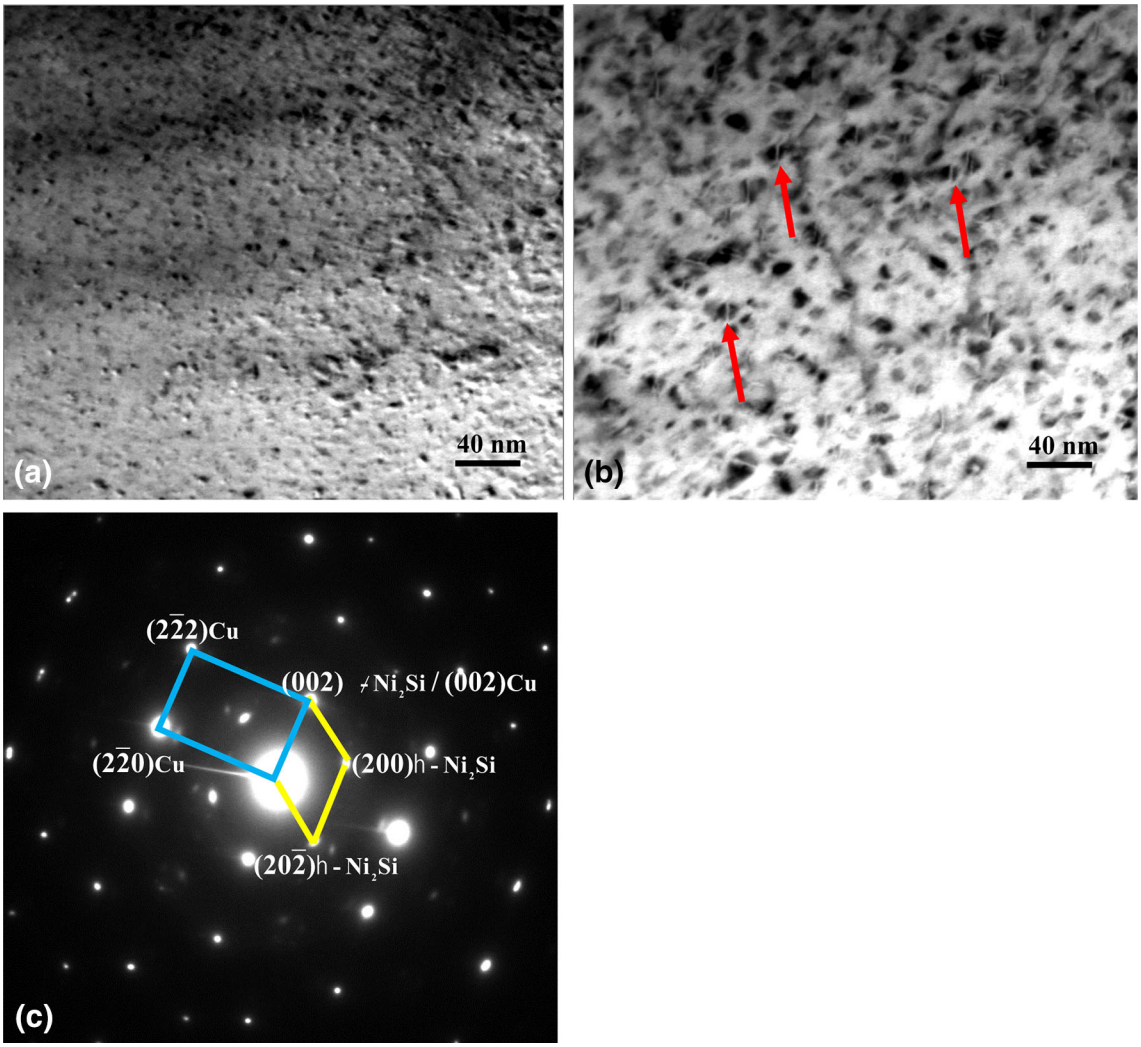

Fig. 5 TEM micrographs of the Cu-Ni-Si-P alloy aged at 450 °C for: (a) 2 h; (b) 48 h; (c) selected area diffraction pattern from (b)

0.05. Therefore, the orientation relationship between $(002)_{Cu}$ and $(002)_{\delta-Ni_2Si}$ is semi-coherent after 48 h of aging. The precipitated phase coarsening was inhibited by the small additions of P. The precipitate's misfit value of the Cu-2.4Ni-0.7Si-0.4Cr alloy was calculated in Ref 24. It is much higher than in the present study for the similar aging process. The present study shows that the addition of P can increase the hardness of the solution-treated Cu-Ni-Si alloy during aging. It can also effectively improve the alloy strength.

4. Discussion

Compared with the Cu-2.0Ni-0.5Si alloy studied by Zhang et al. (Ref 25), the addition of P has important effects on the alloy aging behavior. Figure 7(a) and (b) shows the microstructure of the Cu-Ni-Si and Cu-Ni-Si-P alloys after solution treatment, where the P addition can evidently refine the grain.

Figure 8 shows the strength and conductivity curves of the Cu-Ni-Si and Cu-Ni-Si-P alloys aged at the following processing conditions: 40% cold rolled+aging at 450 °C and 2 h+40% cold rolled+aging at 450 °C. According to Fig. 8(a), the Cu-Ni-Si and Cu-Ni-Si-P alloys show the peak strength of 724 and 804 MPa when aged at 450 °C and 0.5 h, respectively. Comparing the peak strength of the two alloys, the peak strength was increased by 10% with P addition. Due to the overaging, the strength decreased very fast after reaching the peak strength, as shown in Fig. 8(a). At the same aging conditions in Fig. 8(b), the conductivity of the Cu-Ni-Si and Cu-Ni-Si-P alloys is 45% IACS and 49% IACS, respectively. The conductivity also increased by 8.2% with P addition. According to the above analysis, it can be concluded that the addition of P can effectively refine the grain size of the Cu-Ni-Si alloy. The Cu-Ni-Si-P alloy can gain excellent mechanical properties with strength of 804 MPa and conductivity of 49% IACS after 40% cold rolling and aging at 450 °C for 2 h, followed by 40% cold rolling and aging at 450 °C for 0.5 h.

5. Conclusions

After aging at 450 °C for 2 h with 80% cold rolling, Cu-Ni-Si-P alloy achieved excellent combined properties: 551 MPa tensile strength, 226 HV hardness, and 36% IACS electrical

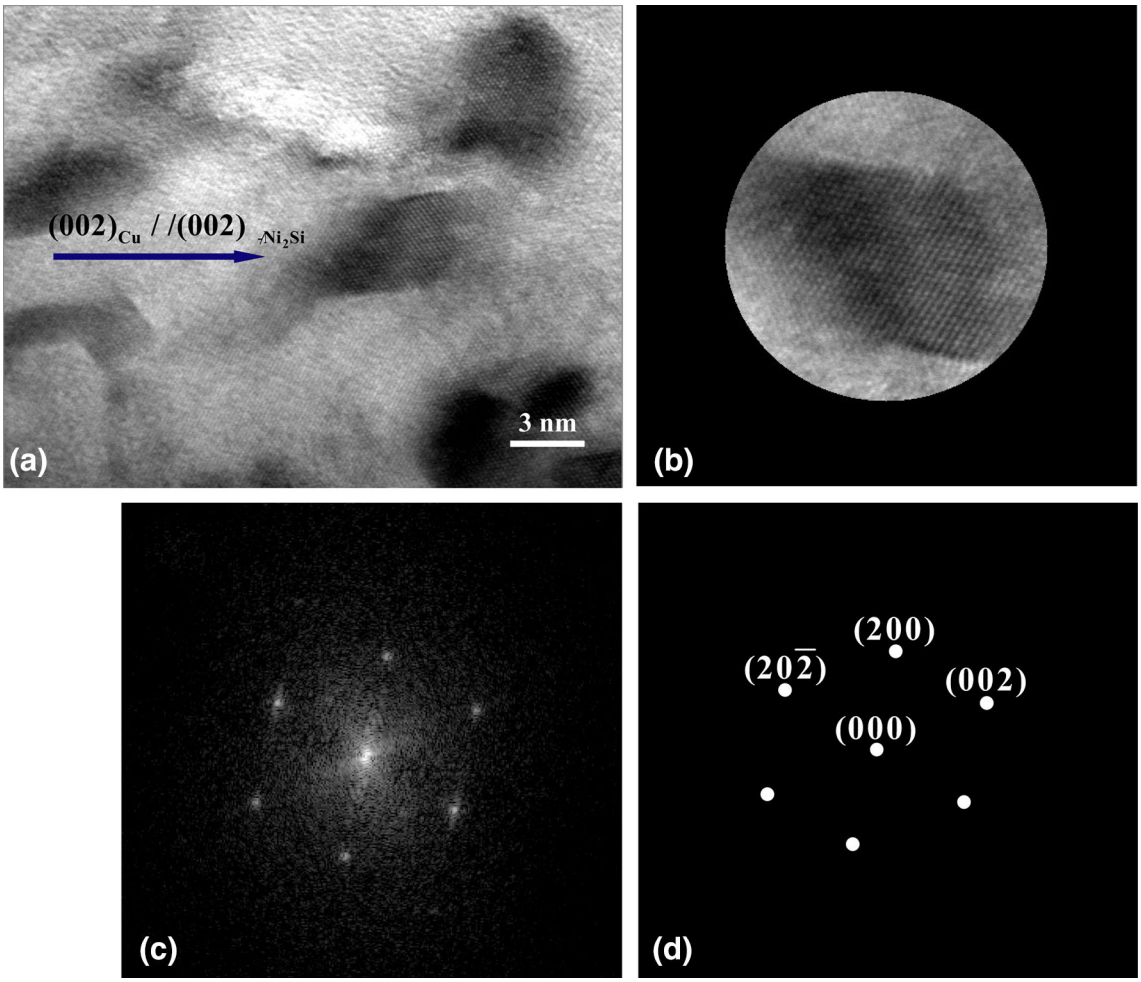

Fig. 6 HRTEM images and corresponding Fourier transform patterns of the alloy aged at 450 °C for 48 h

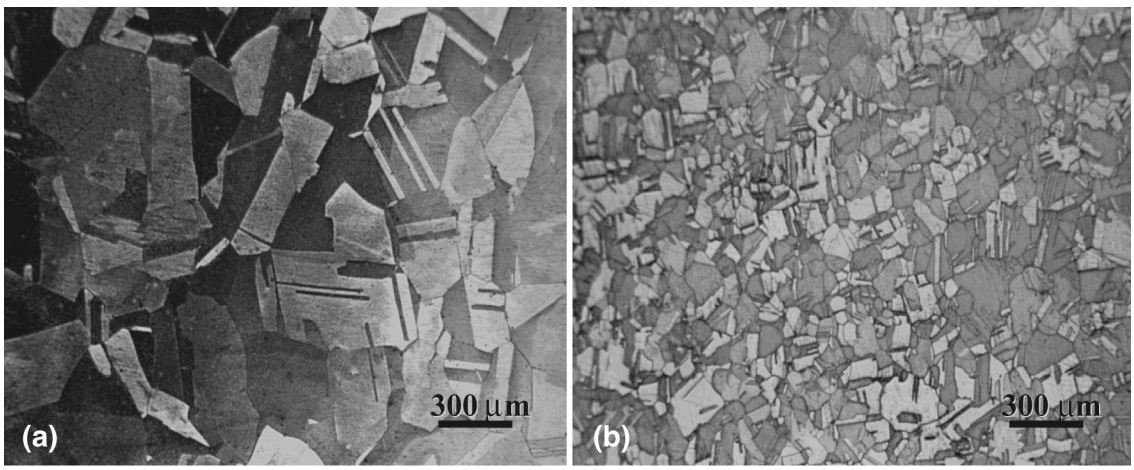

Fig. 7 Microstructure of (a) Cu-Ni-Si and (b) Cu-Ni-Si-P alloys after solution treatment at 950 °C for 1 h

conductivity. Nano-scale δ-Ni_2Si particles precipitated in the alloy after aging for 48 h at 450 °C. The increase in strength and hardness after aging is attributed to the precipitation of fine δ-Ni_2Si particles. The morphology of the fracture surface with a typical ductile fracture pattern appeared in the Cu-Ni-Si-P alloy. The addition of P refined the microstructure and increased the nucleation rate of the precipitates, inhibited the precipitated phase coarsening and effectively enhanced the strength and hardness. The Cu-Ni-Si-P alloy can gain excellent mechanical properties with 804 MPa strength and 49% IACS conductivity

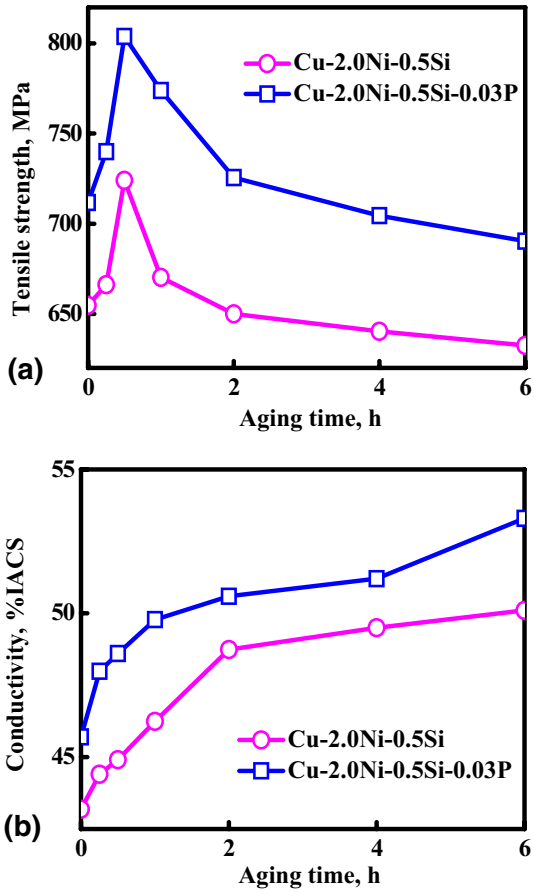

Fig. 8 (a) Tensile strength and (b) conductivity of the Cu-Ni-Si and Cu-Ni-Si-P alloys after 40% cold rolling and aging at 450 °C for 2 h, followed by additional 40% cold rolling and aging at 450 °C for 0.5 h

after aging at 450 °C for 2 h, followed by cold rolling and additional aging at 450 °C for 0.5 h.

Acknowledgment

This work was supported by the National Natural Science Foundation of China (51101052) and the National Science Foundation (IRES 1358088).

References

1. Y. Zhang, A.A. Volinsky, H.T. Tran, Z. Chai, P. Liu, and B.H. Tian, Effects of Ce Addition on High Temperature Deformation Behavior of Cu-Cr-Zr Alloys, *J. Mater. Eng. Perform.*, 2015, **24**, p 3783–3788
2. S.G. Jia, X.M. Ning, P. Liu, M.S. Zheng, and G.S. Zhou, Age Hardening Characteristics of Cu-Ag-Zr Alloy, *Met. Mater. Int.*, 2009, **15**, p 555–558
3. S. Chenna Krishna, N.K. Gangwar, A.K. Jha, B. Pant, and K.M. George, Enhanced Strength in Cu-Ag-Zr Alloy by Combination of Cold Working and Aging, *J. Mater. Eng. Perform.*, 2014, **23**, p 1458–1464
4. L.M. Bi, P. Liu, X.H. Chen, X.K. Liu, W. Li, and F.C. Ma, Analysis of Phase in Cu-15%Cr-0.24%Zr Alloy, *Trans. Nonferrous Met. Soc. China*, 2013, **23**, p 1342–1348
5. Y.Q. Long, P. Liu, Y. Liu, W.M. Zhang, and J.S. Pan, Simulation of Recrystallization Grain Growth During Re-aging Process in the Cu-Ni-Si Alloy Based on Phase Field Model, *Mater. Lett.*, 2008, **62**, p 3039–3042
6. Y.L. Jia, M.P. Wang, C. Chen, Q.Y. Dong, S. Wang, and Z. Li, Orientation and Diffraction Patterns of δ-Ni2Si Precipitates in Cu-Ni-Si Alloy, *J. Alloys Compd.*, 2013, **557**, p 147–151
7. H. Xie, L. Jia, and Z.L. Lu, Microstructure and Solidification Behavior of Cu-Ni-Si Alloys, *Mater. Charact.*, 2009, **60**, p 114–118
8. S.Z. Han, J.H. Gu, J.H. Lee, Z.P. Que, J.H. Shin, S.H. Lim, and S.S. Kim, Effect of V Addition on Hardness and Electrical Conductivity in Cu-Ni-Si Alloys, *Met. Mater. Int.*, 2013, **19**, p 637–641
9. E. Donoso, R. Espinoza, M.J. Dianez, and J.M. Criado, Microcalorimetric Study of the Annealing Hardening Mechanism of a Cu-2.8Ni-1.4Si (at%) Alloy, *Mater. Sci. Eng., A*, 2012, **556**, p 612–616
10. C. Watanabe and R. Monzen, Coarsening of δ-Ni_2Si Precipitates in a Cu-Ni-Si Alloy, *J. Mater. Sci.*, 2011, **46**, p 4327–4335
11. Y. Zhang, A.A. Volinsky, Q.Q. Xu, Z. Chai, B.H. Tian, P. Liu, and H.T. Tran, Deformation Behavior and Microstructure Evolution of the Cu-2Ni-0.5Si-0.15Ag Alloy During Hot Compression, *Metall. Mater. Trans. A*, 2015, **46**, p 5871–5876
12. Q. Lei, Z. Li, M.P. Wang, L. Zhang, Z. Xiao, and Y.L. Jia, The Evolution of Microstructure in Cu-8.0Ni-1.8Si-0.15 Mg Alloy During Aging, *Mater. Sci. Eng., A*, 2010, **527**, p 6728–6733
13. S.C. Krishna, J. Srinath, A.K. Jha, B. Pant, S.C. Sharma, and K.M. George, Microstructure and Properties of a High-Strength Cu-Ni-Si-Co-Zr Alloy, *J. Mater. Eng. Perform.*, 2013, **22**, p 2115–2120
14. X.P. Xiao, B.Q. Xiong, Q.S. Wang, G.L. Xie, L.J. Peng, and G.X. Huang, Microstructure and Properties of Cu-Ni-Si-Zr Alloy After Thermo Mechanical Treatments, *Rare Met.*, 2013, **32**, p 144–149
15. L. Shen, Z. Li, Z.M. Zhang, Q.Y. Dong, Z. Xiao, Q. Lei, and W.T. Qiu, Effects of Silicon and Thermo-Mechanical Process on Microstructure and Properties of Cu-10Ni-3Al-0.8Si Alloy, *Mater. Des.*, 2014, **62**, p 265–270
16. D.M. Zhao, Q.M. Dong, P. Liu, B.X. Kang, J.L. Huang, and Z.H. Jin, Aging Behavior of Cu-Ni-Si Alloy, *Mater. Sci. Eng., A*, 2003, **361**, p 93–99
17. C.D. Xia, Y.L. Jia, W. Zhang, K. Zhang, Q.Y. Dong, G.Y. Xu, and M. Wang, Study of deformation and Aging Behaviors of a Hot Rolled-Quenched Cu-Cr-Zr-Mg-Si Alloy During Thermo-Mechanical Treatments, *Mater. Des.*, 2012, **39**, p 404–409
18. D.M. Zhao, Q.M. Dong, P. Liu, B.X. Kang, J.L. Huang, and Z.H. Jin, Structure and Strength of the Age Hardened Cu-Ni-Si Alloy, *Mater. Chem. Phys.*, 2003, **79**, p 81–86
19. J.Y. Cheng, B.B. Tang, F.X. Yu, and B. Shen, Evaluation of Nanoscaled Precipitates in a Cu-Ni-Si-Cr Alloy During Aging, *J. Alloys Compd.*, 2014, **614**, p 189–195
20. Q. Lei, Z. Li, C. Dai, J. Wang, X. Chen, J.M. Xie, W.W. Yang, and D.L. Chen, Effect of Aluminum on Microstructure and Property of Cu-Ni-Si Alloys, *Mater. Sci. Eng., A*, 2013, **572**, p 65–74
21. I. Altenberger, H.A. Kuhn, M. Gholami, M. Mhaede, and L. Wagner, Ultrafine-Grained Precipitation Hardened Copper Alloys by Swaging or Accumulative Roll Bonding, *Metals*, 2015, **5**, p 763–776
22. S.A. Lockyer and F.W. Noble, Precipitate Structure in a Cu-Ni-Si Alloy, *J. Mater. Sci.*, 1994, **29**, p 218–226
23. Q. Lei, Z. Li, M.P. Wang, L. Zhang, S. Gong, Z. Xiao, and Z.Y. Pan, Phase Transformations Behavior in a Cu-8.0Ni-1.8Si Alloy, *J. Alloys Compd.*, 2011, **509**, p 3617–3622
24. T. Hu, J.H. Chen, J.Z. Liu, Z.R. Liu, and C.L. Wu, The Crystallographic and Morphological Evolution of the Strengthening Precipitates in Cu-Ni-Si Alloys, *Acta Mater.*, 2013, **61**, p 1210–1219
25. Y. Zhang, P. Liu, B.H. Tian, S.G. Jia, and Y. Liu, Study on Aging Kinetics of Cu-2.0Ni-0.5Si Alloy, *J. Funct. Mater.*, 2010, **41**, p 1827–1830